

This document was prepared in conjunction with work accomplished under Contract No. DE-AC09-96SR18500 with the U.S. Department of Energy.

This work was prepared under an agreement with and funded by the U.S. Government. Neither the U. S. Government or its employees, nor any of its contractors, subcontractors or their employees, makes any express or implied: 1. warranty or assumes any legal liability for the accuracy, completeness, or for the use or results of such use of any information, product, or process disclosed; or 2. representation that such use or results of such use would not infringe privately owned rights; or 3. endorsement or recommendation of any specifically identified commercial product, process, or service. Any views and opinions of authors expressed in this work do not necessarily state or reflect those of the United States Government, or its contractors, or subcontractors.

CORROSION OF LEAD SHIELDING IN NUCLEAR MATERIALS PACKAGES

K. H. Subramanian
Savannah River National Laboratory
Bldg 773-A, D-1123
Aiken SC 29808

K. A. Dunn
Savannah River National Laboratory
Bldg 773-41A, Rm. 182
Aiken SC 29808

J. L. Murphy
Savannah River National Laboratory
Bldg 773-41A, Rm. 157
Aiken SC 29808

ABSTRACT

Inspection of United States-Department of Energy (US-DOE) model 9975 nuclear materials shipping package revealed corrosion of the lead shielding that was induced by off-gas constituents from organic components in the package. Experiments were performed to determine the corrosion rate of lead when exposed to off-gas or degradation products of these organic materials. The results showed that the room temperature vulcanizing (RTV) sealant was the most corrosive organic species used in the construction of the packaging, followed by polyvinyl acetate (PVAc) glue. Fiberboard material, also used in the construction of the packaging induced corrosion to a much lesser extent than the PVAc glue and RTV sealant, and only in the presence of condensed water. The results indicated faster corrosion at temperatures higher than ambient and with condensed water. In light of these corrosion mechanisms, the lead shielding was sheathed in a stainless steel liner to mitigate against corrosion.

Figure Captions

Figure 1: 9975 Package Isometric	1
Figure 2: Lead Shielding Coated with White Materials	2
Figure 3: XRD Pattern for White Flake.	3
Figure 4: TGA-MS of Cane Fiberboard Sample Indicating Physiosorbed Water Content	4
Figure 5: Perforated Base Stud Coupon Rack and Lead Coupon	5
Figure 6: Corrosion Rates for Lead Coupons Exposed to Condensed Water Cells at Room Temperature for Continuous Duration of Exposure	6
Figure 7: Corrosion Rates for Lead Coupons to Condensed Water Cells at 50°C for Continuous Duration of Exposure	7
Figure 8: Corrosion Rates for Lead Coupons Exposed to Condensed Water Cells at 75°C for Continuous Duration of Exposure	8
Figure 9: Corrosion Rates for Lead Coupons Exposed to Condensed Water Cells at Room Temperature for Re-Exposed Coupons and Continuously Exposed 120-Day Coupons	9
Figure 10: Corrosion Rates for Lead Coupons Exposed to Condensed Water Cells at 50°C for Re-Exposed Coupons and Continuously Exposed 120-Day Coupons	10
Figure 11: Corrosion Rates for Lead Coupons Exposed to Condensed Water Cells at 75°C for Re-Exposed Coupons and Continuously Exposed 120-Day Coupons	11
Figure 12: Corrosion Rates for Lead Coupons Exposed to Ambient Humidity Cells at Room Temperature for Re-Exposed Coupons and Continuously Exposed 120-Day Coupons	12
Figure 13: Corrosion Rates for Lead Coupons Exposed to Condensed Water Cells at 50°C for Re-Exposed Coupons and Continuously Exposed 120-Day Coupons	13
Figure 14: Corrosion Rates for Lead Coupons Exposed to Condensed Water Cells at 75°C for Re-Exposed Coupons and Continuously Exposed 120-Day Coupons	14

INTRODUCTION

The United States Department of Energy (US-DOE) model 9975 package is a certified package for shipping of nuclear materials in the USA. The 9975 package design includes two nested stainless steel containment vessels designed and fabricated in accordance with Section III of the ASME Boiler & Pressure Vessel Code. The 9975 package design also includes a lead shield around the containment vessels to lower the package surface dose rate.

9975 Package Configuration

The 9975 package is shown in Figure 1 with the materials of construction for each of the major features listed in Table 1.

The primary containment vessel (PCV), secondary containment vessel (SCV), and the outer drum are made of 304L-stainless steel. The containment vessels are placed in a shielding body made of lead which, in turn, is encased in the cane-fiberboard/PVAc laminate comprised of the upper and lower sub-assemblies. The cane-fiberboard, which adheres to ASTM C208-95:Type IV, Grade I wall sheathing, provides three safety functions: thermal insulation to limit PCV/SCV temperature during a fire, mechanical resistance to package crushing, and criticality. Layers of the cane-fiberboard are laminated together with wood glue, a water-based polyvinyl acetate (PVAc) glue. The cane-fiberboard, per the ASTM standard, is nominally composed of cellulose ($\leq 96\%$), starch ($\leq 10\%$), clay ($\leq 2\%$), carbon black ($< 0.5\%$), paraffin wax binder ($\leq 2\%$) and a lamination adhesive ($\leq 3.5\%$). The air shield is attached to the cane-fiberboard insulation sub-assembly with a room temperature vulcanizing (RTV) silicone sealant.

Table 1: Primary Materials of Construction of 9975 Package

<u>Component</u>	<u>Material</u>
Drum	Stainless Steel 304L
Insulation	Cane fiberboard/PVAc
Shielding	ASTM B749 Lead ⁽¹⁾
Shield Liner	Stainless Steel 304
Secondary Containment Vessel (SCV)	Stainless Steel 304L
Primary Containment Vessel (PCV)	Stainless Steel 304L

The cane-fiberboard/PVAc laminate is layered axially within the stainless drum. In this orientation, the outer surface of the lead cylinder is exposed to the laminate edge. The top of the lead shielding body is an aluminum lid which contacts the aluminum bearing plate in the top insulation sub-assembly.

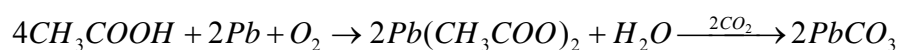
Corrosion Mechanism

Inspections of several 9975 packages revealed a white coating on the exterior surface of the lead shielding, as shown in Figure 2. X-ray diffraction (XRD) analysis taken from a white flake embedded in the cane-fiberboard revealed lead carbonate (cerrusite, PbCO_3) and basic lead carbonate (hydrocerrusite, $\text{Pb}_3(\text{CO}_3)_2(\text{OH})_2$), typically indicative of corrosion of lead by acetic acid.⁽²⁾ Although lead is highly resistant to corrosion in many environments due to the insolubility and self-healing nature of its primary protective film, PbO , lead is known to be susceptible to corrosion in the presence of acetic and chloroacetic, oxalic acid, and formic acids.⁽³⁾ In this case, acetic acid is the specific corrodant of interest because the RTV, PVAc, and the cellulosic organic materials can off-gas acetic acid due to completion of the curing process of subsequent environmental degradation.

The corrosion products of cerrusite/hydrocerrusite determined by XRD are consistent

with corrosion by acetic acid, in the presence of carbon dioxide, as shown in Equation 1. Acetic acid reacts with lead to produce lead acetate and lead hydroxide, which in turn react with carbon dioxide and form lead carbonate or basic lead carbonate. Lead carbonate then releases acetic acid and the process becomes self-sustaining.⁽⁴⁾ In fact, the traditional method of formulating “white lead” (basic lead carbonate) for use as a white pigment, i.e. the “Dutch process”, is to expose lead to acetic acid.⁽⁵⁾

Equation 1: Acetic Acid Corrosion of Lead ⁽⁶⁾



The corrosion of the lead shielding in the 9975 package is thought to be primarily atmospheric in nature, or under thin films, as opposed to an immersed condition. The unexpected corrosion of lead due to acetic acid has been primarily reported in the context of atmospheric corrosion as seen in the museum and artifact preservation community.⁽⁷⁾ However, as with all atmospheric corrosion mechanisms, this is a complex function of the condensate on the lead material. The acetic acid condenses in an aqueous surface film leading to the formation of lead acetate/lead hydroxide, which subsequently reacts with carbon dioxide to form lead carbonates. The subsequent formation and migration of the lead acetate/hydroxide compounds into the cracks of the carbonate layer towards the metal surface leads to the dissolution of the PbO under layer, the oxidation of lead, and subsequent peeling of the carbonate layer. The corrosion of lead reacting with acetic acid is typically a self-sustaining process because the reaction of the lead acetate/hydroxides with carbon dioxide to form lead carbonate releases acetic acid thereby sustaining the corrosion processes.⁽⁴⁾

Several key data are necessary for the verification of the corrosion hypothesis and to model the short-term and long-term impact of the lead shielding corrosion on the performance of

the model 9975 package. These key data include the corrosion rate of lead when exposed to an environment similar to that of a 9975 package. These exposure experiments have been conducted and the results are presented here.

EXPERIMENTAL APPROACH

The experimental approach focused on the effect of the acetic acid emissions from organic components of the model 9975 package on the corrosion of lead. The testing included analysis of the corrosion of the lead as a function of the aging of the organic materials. Due to the geometry of the package and the location of the corrosion the cane-fiberboard, PVAc glue, and the silicone were suspected to be involved in the corrosion process, with each a known potential source of the acetic acid. The corrosion may occur in ambient humidity conditions or under conditions that allow condensation in the package.

Experimental Test Matrix

The experimental matrix, summarized in Table 2, was a parametric combination of the following discrete variables: (1) configuration of the organic materials, (2) temperature, (3) humidity, and (4) duration of exposure. The configurations of the organic materials included each organic constituent uniquely to isolate their effects on the corrosion rate as well as combinations to represent the most likely exposures in the model 9975 package.

Table 2: Summary of Discrete Variables in Parametric Test Matrix

<u>Configuration of Organic Materials</u> <ol style="list-style-type: none"> 1. Cane Fiberboard (CF) 2. PVAc Glue 3. RTV sealant 4. CF + Glue 5. CF + Glue + RTV 	<u>Temperature</u> <ol style="list-style-type: none"> 1. Ambient 2. 50°C 3. 75°C
<u>Humidity</u> <ol style="list-style-type: none"> 1. Ambient 2. Condensed Water 	<u>Duration of Exposure (days)</u> <ol style="list-style-type: none"> 1. 30 2. 75 3. 120

Each of the discrete variables for exposure of the coupons was chosen on the basis of their influence on the corrosion of lead. The testing was performed by exposing lead coupons, conforming to the ASTM B749 Standard, to the various combinations of the discrete variables to determine the effect of each as well as synergistic effects. The temperatures tested covered the expected boundary conditions in the model 9975 package. The effect of humidity was tested by exposure to ambient conditions and with a small amount of condensed water thereby creating a 100% relative humidity environment. The CF materials were not dried prior to the exposure testing and any moisture retained was allowed to react. This is consistent with the package construction practices. The corrosion rates were calculated for the various durations of exposure to determine any changes in corrosion rates. Additionally, the coupons exposed to 30/75 days and analyzed were then placed back into exposure to simulate the opening and closing of the packages and potentially replenishing the carbon dioxide supply to further support the corrosion reaction.

The condition considered bounding, but most representative, of the package condition was expected to be the coupon exposed to the CF/glue organic exposed in the ambient humidity condition. The CF/glue laminate in the package is nearly in intimate contact with the lead

shielding as in the test setup and is considered a bounding condition due to the following:

1. The experiments were done in small volume containers with a relatively large lead coupon and organic materials surface areas exposed for corrosion processes with little airspace for dissipation/dilution of acetic acid vapors.
2. The extremely aggressive PVAc glue in the experimental setup was relatively large in volume as well as incompletely cured.
3. The opening and closing of the package will allow the acetic acid vapor to escape thereby temporarily stalling the corrosion process, while replenishing the carbon dioxide and moisture required to support the reaction.

Each of the organic constituents is a known source of acetic acid vapor either from the curing process or due to degradation processes, primarily hydrolysis. A description of the organic constituents and their effects on the corrosion of lead are given in the following sections.

Cane-Fiberboard (CF)

The cane-fiberboard materials used for testing were cut from a model 9975 package spare parts assembly, and were nominally composed of cellulose ($\leq 96\%$), starch ($\leq 10\%$), clay ($\leq 2\%$), carbon black ($< 0.5\%$), paraffin wax binder ($\leq 2\%$). A compositional and thermal characterization of the CF using energy dispersive spectroscopy (EDS), inductively coupled plasma-mass spectroscopic analysis (ICP-MS), and ion chromatography (IC), as been completed by Ortiz, et.al.⁽⁸⁾ The analysis showed the presence of aluminum, silicon, sulfur, titanium, iron with significant potassium and calcium. The major anions present were fluoride, chloride, bromide and sulfate. The chloride concentration was measured at 960 $\mu\text{g/g}$ whereas in other studies it has been measured up to 1800 $\mu\text{g/g}$, both of which are a function of leaching parameters used.⁽⁹⁾ Both studies indicated that the actual chloride concentration may be much higher, certainly

sufficient to cause corrosion of the stainless steel outer drum if leached. If the conditions were to support significant condensation, chloride is expected to leach out causing corrosion of the stainless steel drum, which was not evident in this case. As such, this suggests that chlorine has not leached from the CF indicating minimal condensation, if any. However the reaction rates to produce acetic acid vs. chloride leaching is unknown.

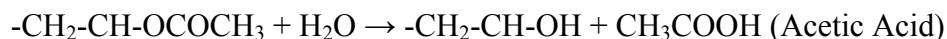
Since the primary constituent of CF is cellulose, a survey of wood as a surrogate was undertaken to determine the potential reactions of hemicellulose to create acetic acid. Wood materials are known to emit acetic acid vapor as a function of hemicellulose hydrolysis.⁽¹⁰⁾ The extent of the vapor emission is a function of the initial acetic acid concentration as well as cellulose concentration.⁽¹¹⁾ The impact of the acetic acid vapor emissions from wood on the corrosion of lead is widely known and addressed in the museum and artifact industry since the preservation of lead artifacts in wood casings has resulted in extensive corrosion. In fact, the Oddy test uses lead exposure to wood to determine the extent of acid vapor emission from specific casing designs for museum applications.⁽¹²⁾

Polyvinyl Acetate (PVAc)

The PVAc glue is a water-based thermoplastic adhesive commonly used as an emulsion of PVAc polymers in water. It is formed by polymerization of vinyl monomers in water and then cures by evaporation of water. PVAc creates strong bonds in wood but is not moisture or heat resistant unless cross-linked which consequently lowers the quality of adhesion.⁽¹³⁾ The PVAc tested was not cross-linked and therefore softens at elevated temperatures and is less resistant to moisture and humidity than thermosetting resins.⁽¹³⁾

Another key facet of the PVAc is the availability of free hydroxyl groups since PVAc is polymerized with minor amounts of vinyl alcohol, than can be formed by hydrolysis of the

acetate groups. Vinyl acetate, the monomer for PVAc polymerization, is also produced by catalytic oxidative condensation of acetic acid and ethylene.⁽¹⁴⁾ The hydrolysis of the PVAc creates PVOH and acetic acid, per the following reaction which can be accelerated by higher temperatures, and is self catalyzed by the acetic acid.⁽¹⁵⁾



Experience with polyvinyl acetate has led to the recommendation that it also not be used in the museum and artifact preservation industry, because of its corrosivity towards lead in particular.⁽¹⁶⁾

Silicone Based Sealant

The silicone-based sealant is a two-part room temperature vulcanizing (RTV) system which cures via the silicone molecule's silanol ends. Silicone sealants are based on mixtures of fillers (e.g., silica), silicone polymers, cross linking components, and catalysts. The polymer has a siloxane backbone, i.e., Si-O-Si, with alkyl and alkoxy or acetoxy pendant groups. The latter are readily hydrolyzed to silanol groups (SiOH) which form larger chains by condensation and loss of alcohol or acetic acid. When the organic groups polymerize, a volatile species is generally released - the most common being acetic acid. The sealant typically does not continue to off-gas acetic acid when completely cured, but can release acetic acid if it degrades most likely due to hydrolysis.

Water and Carbon Dioxide

It is important to identify the source of the water vapor and the carbon dioxide in the package. The outer drum is not a pressure or leak tight boundary, thereby potentially allowing water vapor and air into the CF assembly. The CF has significant porosity potentially containing humid air providing water as well as the carbon dioxide for the reactions to take place. TGA-MS

analysis, shown in Figure 4, of the CF indicated water physisorbed onto the surface in addition to the humidity. Measurements of the moisture content of CF in the 9975 package shows typical levels of 12-14% wood moisture equivalent to equilibrium with an atmospheric humidity level of 65-75% at 70°F.⁽¹⁷⁾ This is compliance with ASTM Standard C208, “Standard Specification for Cellulosic Fiber Insulating Board”, which allows a maximum water absorption of 7-15% depending upon thickness of the wall sheathing materials.

Experimental Setup

Testing for each unique condition was done in a 125-mL clear glass septa bottle at temperature within an oven. The lead coupons, nominally 3.175 mm, were mounted on a stainless steel rack perforated base stud (Figure 5) with the organic assemblies. The organic assemblies were assembled by cutting individual test materials into a pre-designated pattern for mounting by screw onto the coupon stud. The lead coupon was exposed to the assemblies on both sides but were separated using Teflon washers and nuts to allow for air exchange in the interface and prevent galvanic coupling with the base stud. Coupons were weighed, measured, and photographed before and after exposures.

The coupons were analyzed for corrosion after the exposure testing. The coating thickness was measured with an x-y traveling stage microscope after scraping the edge to reveal the underlying lead coupon with the carbonate coating. This measured coating thickness was used to calculate the corrosion rate.

RESULTS

The coupons were analyzed after completion of their exposures. The coupons that were exposed for 30 and 75 days were re-exposed and analyzed after exposure for 120 days to

simulate the opening and closing of the package. The coupons were initially visually inspected to determine the presence of corrosion product. The coupons were then weighed and dimensioned. The carbonate thickness was measured when possible by scraping a portion of the edge and using an x-y traveling microscopic stage. The corrosion rate was calculated assuming that the carbonate layer consisted of 50% cerrusite and 50% hydrocerrusite, since both were found by XRD analyses. However, relative variations are expected to be minimal due to the minimal variation in the compounds. Using the data shown in Table 3, it was calculated that for 1 μm of lead carbonate, approximately 0.45 μm of lead is lost, and for 1 μm of basic lead carbonate, 0.4 μm of lead is lost. This implies that for every 1 μm of coating thickness, there is 0.425 μm lead lost.

Table 3: Select Properties of Lead, Lead Carbonate, and Basic Lead Carbonate⁽¹⁸⁾

	Lead	Lead Carbonate (cerrusite)	Basic Lead Carbonate (hydrocerrusite)
Chemical Symbol	Pb	PbCO ₃	Pb ₃ (CO ₃) ₂ (OH) ₂
Molecular Weight (g/mol)	207.2	267.2	775.6
Density (g/cm³)	11.34	6.6	6.14
Moles lead consumed per mole of carbonate product	--	1	3

The corrosion rates are all reported as amount of lead metal lost per unit of time. The rates were calculated using the following formula

$$\text{Equation 2: Corrosion Rate Calculation}$$

$$\frac{\text{Coating Thickness}(\mu\text{m})}{\text{Duration}} [0.425] = \frac{\text{Lead Lost}(\mu\text{m})}{\text{Year}}$$

The corrosion rates were calculated for the coupons exposed in the condensed water cell experiments that were exposed for the continuous duration of exposures and also for the coupons that were re-exposed after analysis after the interim 30/75 day exposures. The calculated

corrosion rates are reported in Figure 6 to 14 for each of the temperatures, durations, and organic configurations tested. Visual observations were made on coupons exposed to cells without condensed water, since these coupons did not exhibit measurable corrosion. A discussion of the visual observations follows the sections on corrosion rates.

Corrosion Rate Analysis for the Coupons Exposed in Condensed Water Cells

The corrosion rates (mm/year) for the lead coupons exposed in the condensed water cells for the complete duration of exposure are shown in Figure 6 to 8, for room temperature, 50°C, and 75°C respectively.

The PVAc glue induced corrosion of the lead metal, but did not sustain a linear corrosion rate as would be expected by the self-sustaining reaction. This is hypothesized to be either due to the variability in the degree of initial curing of the PVAc glue when placed into test or the consumption of available reactants during the exposure. The glue sample placed into the 30/75-day test cells was observed to be poorly cured relative to the glue samples placed in the continuous 120-day cell. Since the cells were not opened during the continuous 120-day exposure period, the available CO₂ or H₂O may have been consumed sufficiently to decelerate the corrosion of the lead metal.

Higher temperatures led to higher corrosion rates, as well as measurable corrosion from exposure to only the cane fiberboard. In contrast, room temperature exposure to only the cane-fiberboard led to no measurable corrosion. The corrosion rate of lead when exposed to the PVAc glue did not sustain a linear rate even at the higher temperatures. Exposure to only the RTV led to the highest corrosion rates.

The highest corrosion rate at both of the higher temperatures tested was the CF/Glue/RTV configuration. Judging from the corrosion rate of lead when exposed only to RTV,

it is hypothesized that this corrosion rate may have been induced primarily by the RTV.

The corrosion rate data for the lead coupons exposed to the condensed water cells for the re-exposed coupons are shown in Figure 9 to 11, for exposure at room temperature, 50°C, and 75°C respectively. The continuous 120-day coupons are included for comparison purposes. In contrast to the initial 30-day exposures, re-exposure and replenishment of reactionary species at room temperature induced corrosion in the CF sample for the 30-day test.

Corrosion was seen on all re-exposed coupons at higher temperatures, indicating that replenishment of reactionary species, i.e. CO₂ and H₂O may be a key factor in inducing corrosion of lead in the long-term. This is further corroborated since the re-exposed coupons exhibited higher corrosion rates than the continuous 120-day coupons that were never removed out of test for all organic configurations.

Corrosion Rate Analysis for the Coupons Exposed in Ambient Humidity Cells

The corrosion rates for the ambient humidity cells were measured and calculated when possible. The lead coupons that were initially exposed for the 30/75 day cycles, and then re-exposed, were the only coupons that exhibited any measurable corrosion. The corrosion rate data for the lead coupons exposed to the ambient humidity cells for the re-exposed coupons are shown in Figure 12 to 14, for exposure at room temperature, 50°C, and 75°C respectively. Measurable corrosion occurred on lead coupons exposed to the glue samples in both the 30-day re-exposed coupon and the continuously exposed 120-day coupon.

Exposure of the coupons at higher temperatures led to corrosion of lead coupons exposed to more configurations than exposure at room temperature. In addition, the higher temperatures led to higher corrosion rates. Measurable corrosion occurred on all coupons exposed to the RTV. However, these coupons exhibited much lower (approximately ½) corrosion rates than the

coupons exposed to similar organic configurations with condensed water as described in the previous section.

As previously discussed, the initial integrity of the organic assembly is suspected to play a large role in the corrosion response. The initial integrity of the PVAc glue and the RTV material is dependent upon the degree of curing which can affect the corrosion of the lead since both the PVAc and RTV off-gas acetic acid during polymerization (curing). In addition, the degree of curing controls the ability of each of these materials to resist hydrolysis and the consequent release of acetic acid. Consequently, the corrosion rates for lead are expected to increase if the PVAc or RTV are poorly cured.

SUMMARY DISCUSSION

The experimental test matrix was developed to determine the effect of organic configuration, temperature, humidity and the effect of durations of exposure on the corrosion of lead in a model 9975 nuclear materials package. The corrosion rate data can be used to infer the effect of each of these discrete variables on the lead corrosion response.

The RTV sealant was the most corrosive organic species in the testing. When the organic groups polymerize, a volatile species is generally released - the most common being acetic acid. The RTV in the model 9975 package may contribute to the acetic acid within the package. However, the geometry of the package is such that the RTV is not in intimate contact with the lead nor is it abundant in the design. As such, the other components are the likely major contributors to the corrosion of the lead.

The PVAc glue was the next most aggressive species in the testing. The PVAc glue used for the 9975 assembly is not cross-linked and thus softens as its temperature is raised above room

temperature, and it is less resistant to moisture and humidity than thermosetting resins. The PVAc glue is suspected to be the primary source of acetic acid in the model 9975 package because of its abundance and location near the lead shield. The humidity and the temperatures within the package are sufficient to degrade the PVAc glue, particularly if incompletely cured during the manufacturing process. The PVAc glue is nearly in intimate contact with the lead shielding in the package, with sufficient vapor space in between to allow for build-up of acetic acid emissions. In addition, the CO_2 and H_2O within this vapor space are sufficient to support the corrosion reactions as well as to continue to degrade the PVAc.

The temperature and humidity also had an effect on the corrosion response of the lead. The coupons exhibited faster corrosion at higher temperatures than at room temperatures. There was a pronounced effect of condensed water as the coupons exposed in the cells with condensed water exhibited much higher corrosion rates. This can be specifically compared for the RTV configurations, where the corrosion rates doubled as a function of moisture and temperature.

The corrosion of the lead was also determined to be a function of the duration of exposure. The corrosion rates did not maintain a linear rate per the corrosion mechanism which would have been indicative of a self-sustaining process. This may have been due to the depletion of reactants for the longer exposures or due to the incongruity of the initial condition of the organic samples. Literature data also suggests that replenishment of the acetic acid is necessary for the corrosion reaction to continue.⁽¹⁹⁾ However, only minimal amounts of acetic acid, e.g. 1000ppb, were reported necessary to significantly increase the corrosion rate of lead. In this case, the replenishment of the acetic acid may occur when the packages are open/shut allowing more moisture infiltration and consequently degrade the organic components.

However, the coupons that were re-exposed after opening and closing in specific

situations exhibited higher corrosion than the coupons that had continuous 120-day exposures. This was particularly seen in the ambient humidity conditions, where the moisture content would have been replenished when opened and closed.

CONCLUSIONS AND RECOMMENDATIONS

The data can be used to draw several conclusions on the corrosion of the lead shielding in the model 9975 package. The testing confirmed that the organics of the model 9975 package cause corrosion of the lead shielding through acetic acid emissions. The RTV sealant was determined to be the most aggressive in the experiments, followed by the PVAc glue. In the 9975 package, because the RTV sealant is not in intimate contact with the lead, the PVAc glue was determined to be the most aggressive contributor due to its proximity in the design and its potential for incomplete curing during fabrication of the package. Incompletely cured PVAc glue during package construction will lead to greater acetic-acid emission as it continues to cure in the package or during degradation in the warm, moist environment of the package.

In light of these corrosion mechanisms, the lead shielding was sheathed in a stainless steel liner to mitigate against corrosion. The safety case analyses and documentation are being revised for the additional stainless steel liner.

ACKNOWLEDGEMENTS

The authors gratefully acknowledge Karen R. Hicks for performing the experiments and technician support throughout the project. The author also gratefully acknowledges W.L. Daugherty, T.E. Skidmore, K.J. Imrich, and A. Jurgenson for the technical support and analyses. This research was performed under the auspices of Contract No DE-AC09-96SR18500 with the U.S. Department of Energy.

REFERENCES

1. ASTM B749-03. *Standard Specification for Lead and Lead Alloy Strip, Sheet, and Plate Products*. ASTM International (2003).
2. Subramanian, K.H. *Mechanism for Corrosion of Lead Shielding in Model 9975 Package*. Washington Savannah River Company, WSRC-TR-2005-00193 (2005).
3. Goodwin, F.E. *Uhlig's Corrosion Handbook: Lead and Lead Alloys* (New York: John Wiley & Sons) (2000)
<http://www.knovel.com/knovel2/Toc.jsp?BookID=682&VerticalID=0>.
4. Blackshaw, S.M. and Daniels, V.D. *Testing of Materials for Use in Storage and Display in Museums*. The Conservator 3(18), (1979).
5. Calvert, J.B. *Lead*. University of Denver, Department of Physics, retrieved April 26, 2005, <<http://www.du.edu/~jcalvert/phys/lead.htm>>
6. Edwards, R., Bordass, R., Farrell, D. *Determination of Acetic and Formic Acid in Lead Corrosion Products by Ion-Exchange Chromatography*. Analyst 122, 1517-1520 (1997).
7. Rocca, E., Rapin, C., Mirambet, F. *Inhibition Treatment of the Corrosion of Lead Artifacts in Atmospheric Conditioned and by Acetic Acid Vapor: Use of Sodium Decanoate*. Corrosion Science 46, 653-665 (2004).
8. Diaz-Ortiz, A., et. al. *Characterization of Celotex and Thermodynamic Calculations of the Formation of Corrosion Precursors on Beryllium*. University of Texas at Austin Amarillo National Resource Center for Plutonium, ANRCP-1999-16 (1999).
9. Lillard, R.S., et.al. *Preliminary Investigation into the Corrosion of Beryllium Exposed to Celotex and Water*. Los Alamos National Laboratory, LA-UR# 97-0859 (1997).

10. Arni, P.C., et. al. *The Emission of Corrosion Vapours by Wood:I. Survey of the Acid-Release Properties of Certain Freshly Felled Hardwoods and Softwoods*. Journal of Applied Chemistry 15, 305-313 (1965).
11. Arni, P.C., et. al. *The Emission of Corrosion Vapours by Wood:II. The Analysis of the Vapours Emitted by Certain Freshly Felled Hardwoods and Softwoods by Gas Chromatography and Spectrophotometry*. Journal of Applied Chemistry 15, 463-468 (1965).
12. Oddy, W.A. *An Unexpected Danger in Display Museums* Journal 173, 27-28 (1973).
13. Petrie, E.M. *Handbook of Adhesives and Sealants* (New York: McGraw-Hill) (2000).
14. Carraher, C.E., and Seymour, R.B. *Polymer Chemistry* (Boca Raton: CRC Press) (2000).
15. Wheeler, O.L., et. al. *Molecular Weight Degradation of Polyvinyl Acetate on Hydrolysis* Journal of Polymer Science 8(4), 409-423 (2003).
16. Storch, P.S. *Exhibit and Materials Storage Handbook: Test Results Index and Materials Glossary*. (Minnesota Historical Society) (2000).
17. Simpson, W.T. *Equilibrium Moisture Content of Wood in Outdoor Locations in the United States and Worldwide*. USDOA – Forestry Service, FPL-RN-0268 (1998).
18. *Handbook of Chemistry and Physics*. (Boca Raton: CRC Press) (1971).
19. Niklasson, A., et. al. *Influence of Acetic Acid Vapor on the Atmospheric Corrosion of Lead*. Journal of the Electrochemical Society 152(12), B519-B525 (2005).

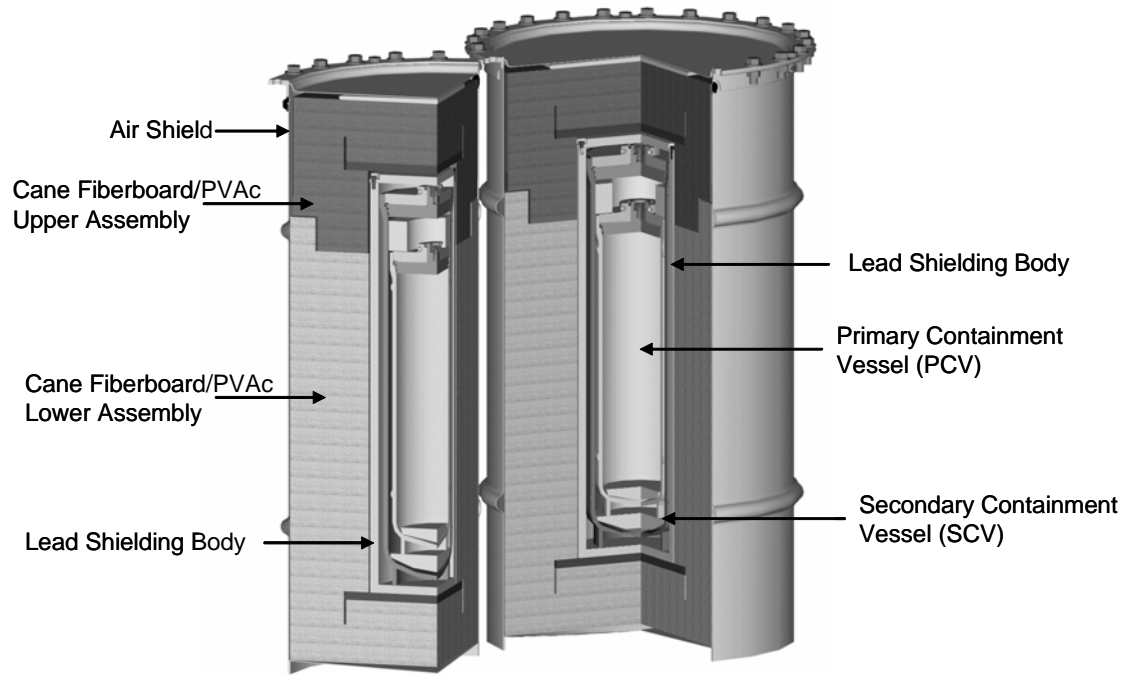


Figure 1: 9975 Package Isometric



Figure 2: Lead Shielding Coated with White Materials

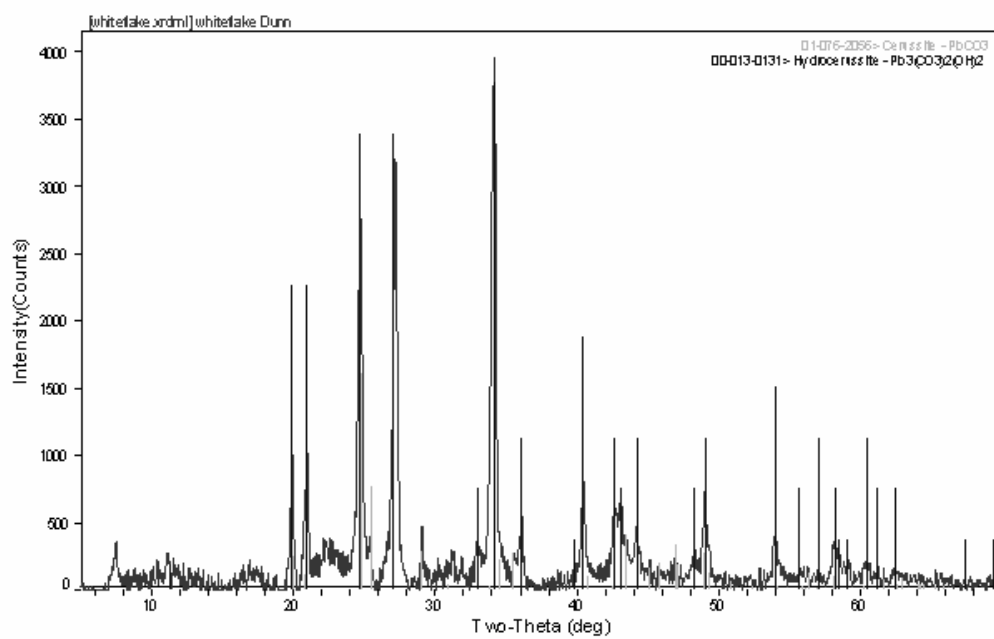


Figure 3: XRD Pattern for White Flake.

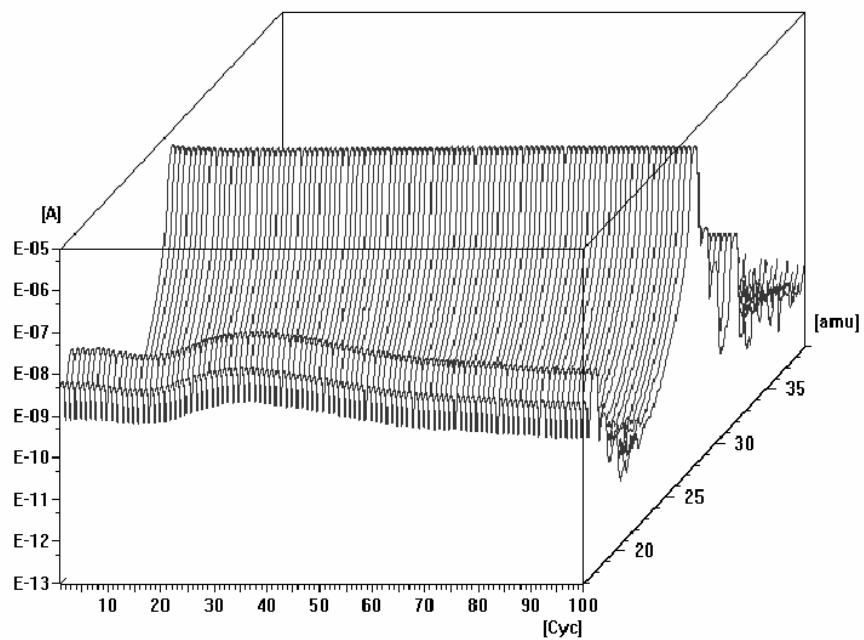


Figure 4: TGA-MS of Cane Fiberboard Sample Indicating Physiosorbed Water Content

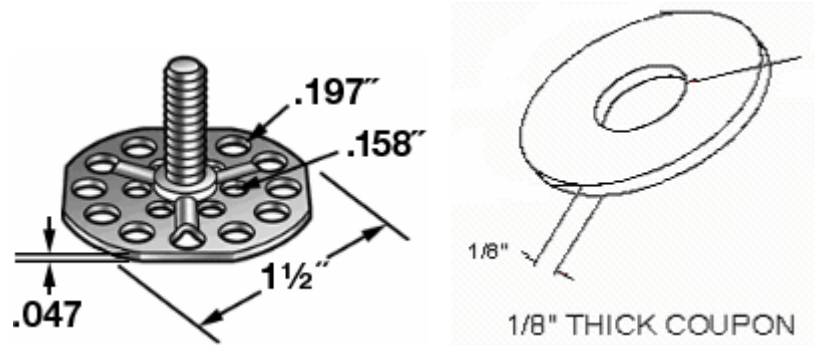


Figure 5: Perforated Base Stud Coupon Rack and Lead Coupon

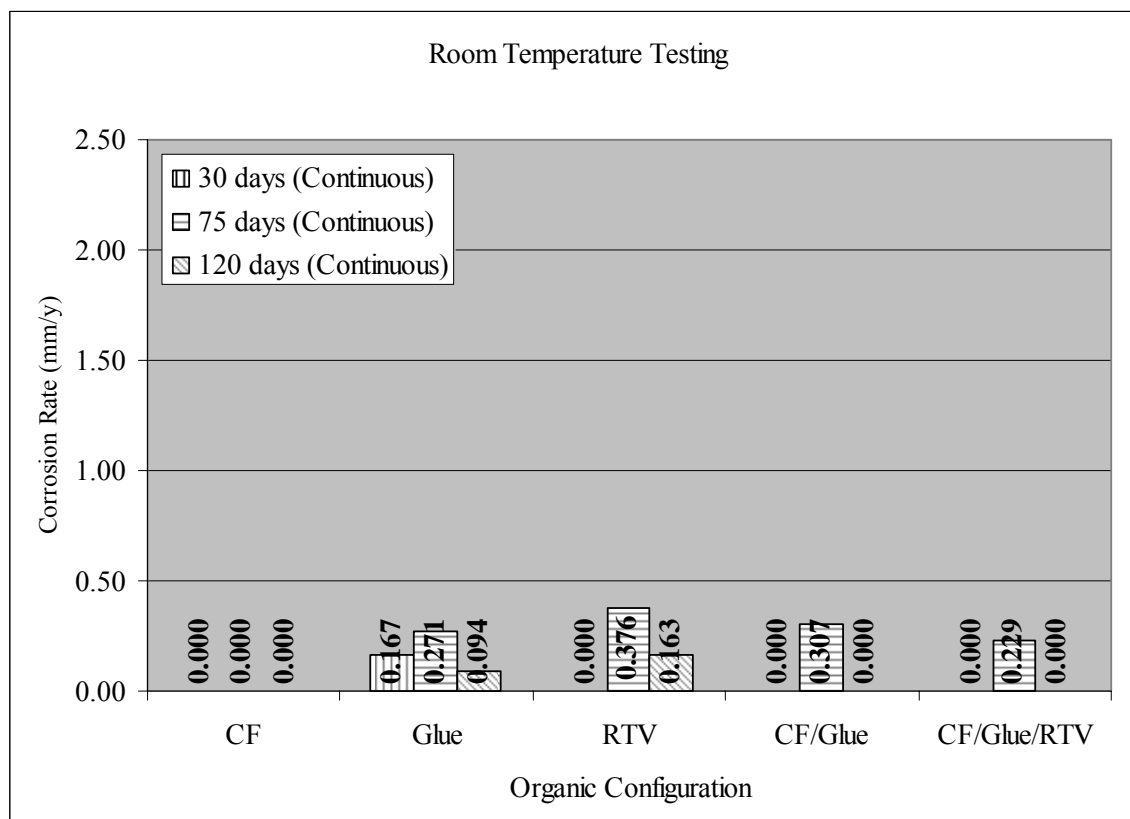


Figure 6: Corrosion Rates for Lead Coupons Exposed to Condensed Water Cells at Room Temperature for Continuous Duration of Exposure

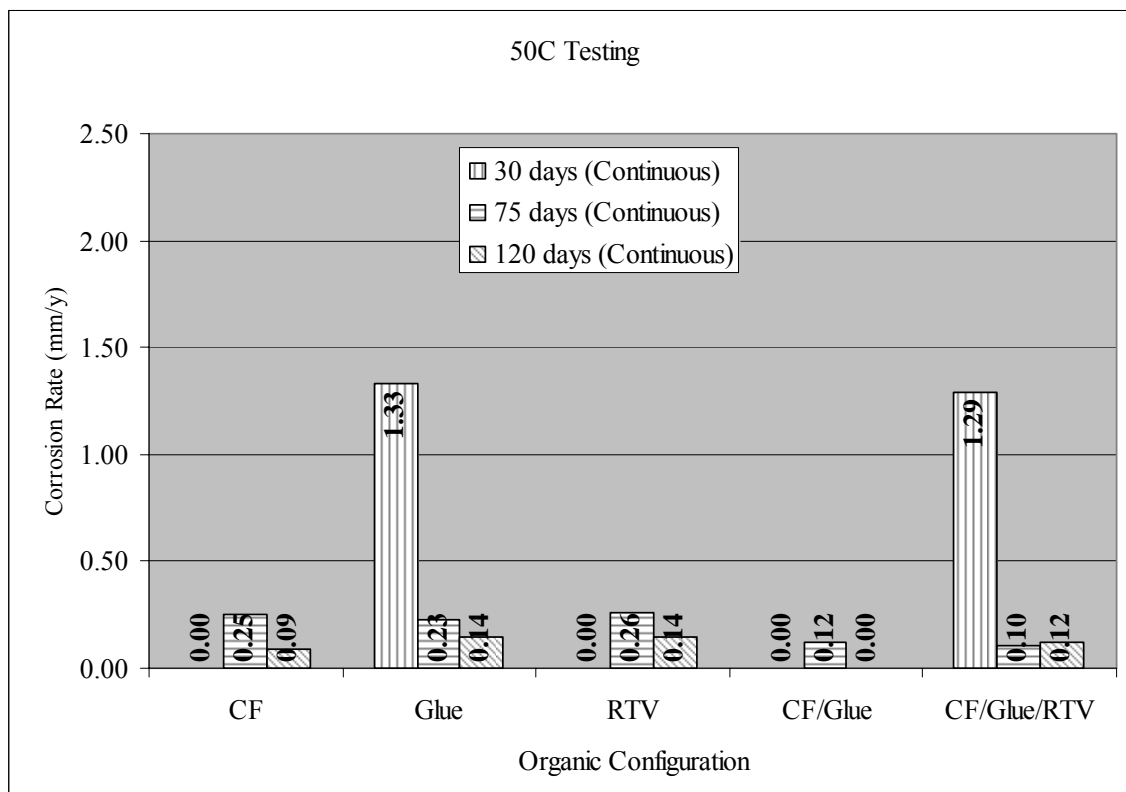


Figure 7: Corrosion Rates for Lead Coupons to Condensed Water Cells at 50°C for Continuous Duration of Exposure

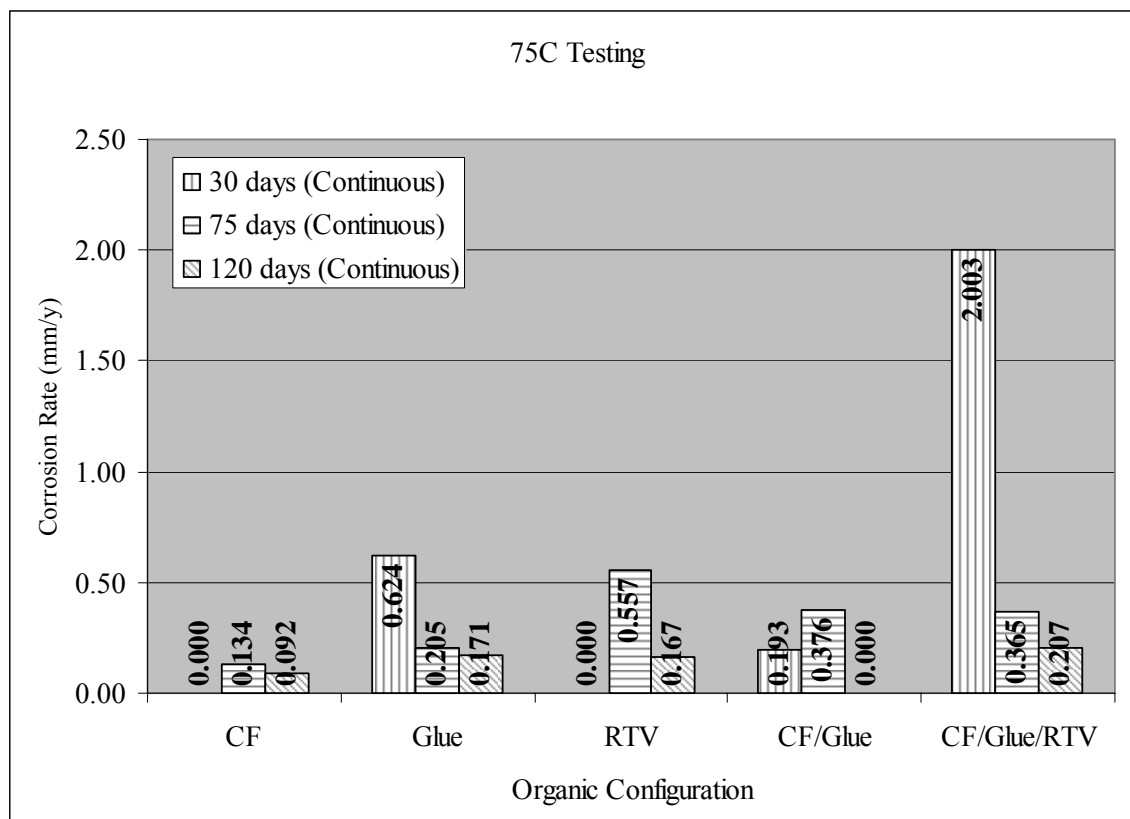


Figure 8: Corrosion Rates for Lead Coupons Exposed to Condensed Water Cells at 75°C for Continuous Duration of Exposure

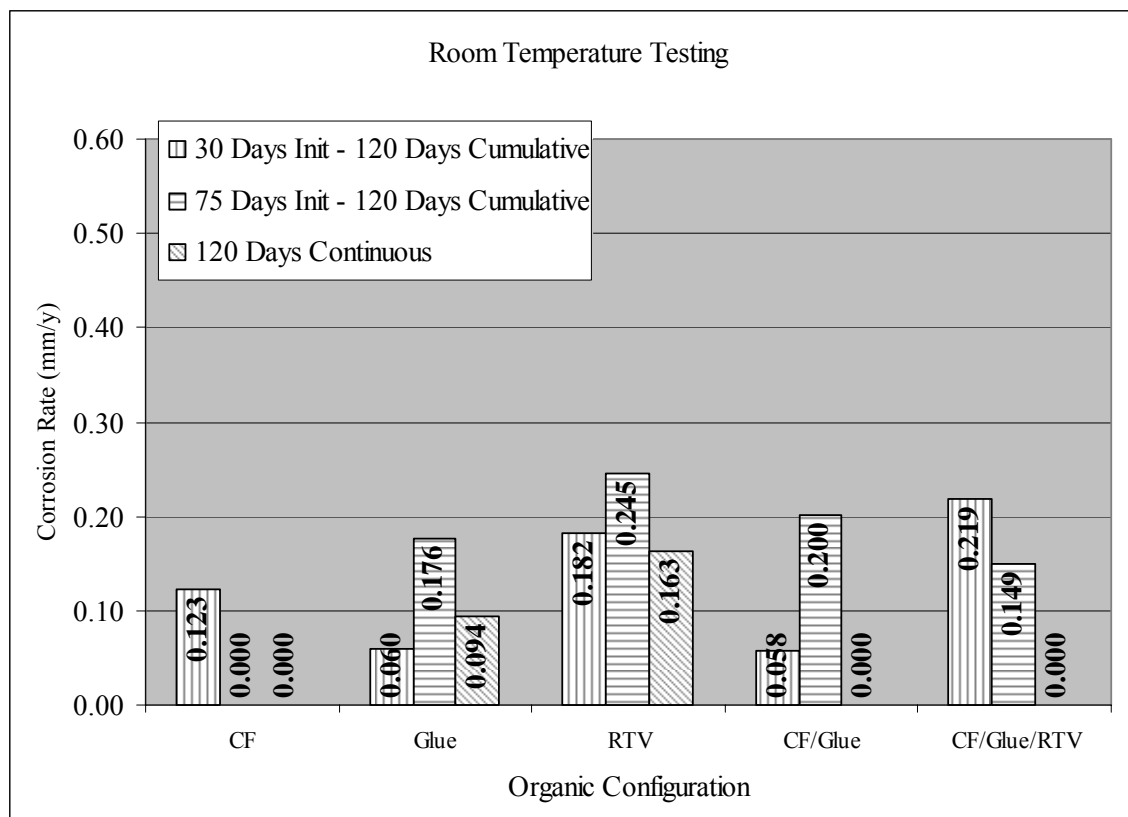


Figure 9: Corrosion Rates for Lead Coupons Exposed to Condensed Water Cells at Room Temperature for Re-Exposed Coupons and Continuously Exposed 120-Day Coupons

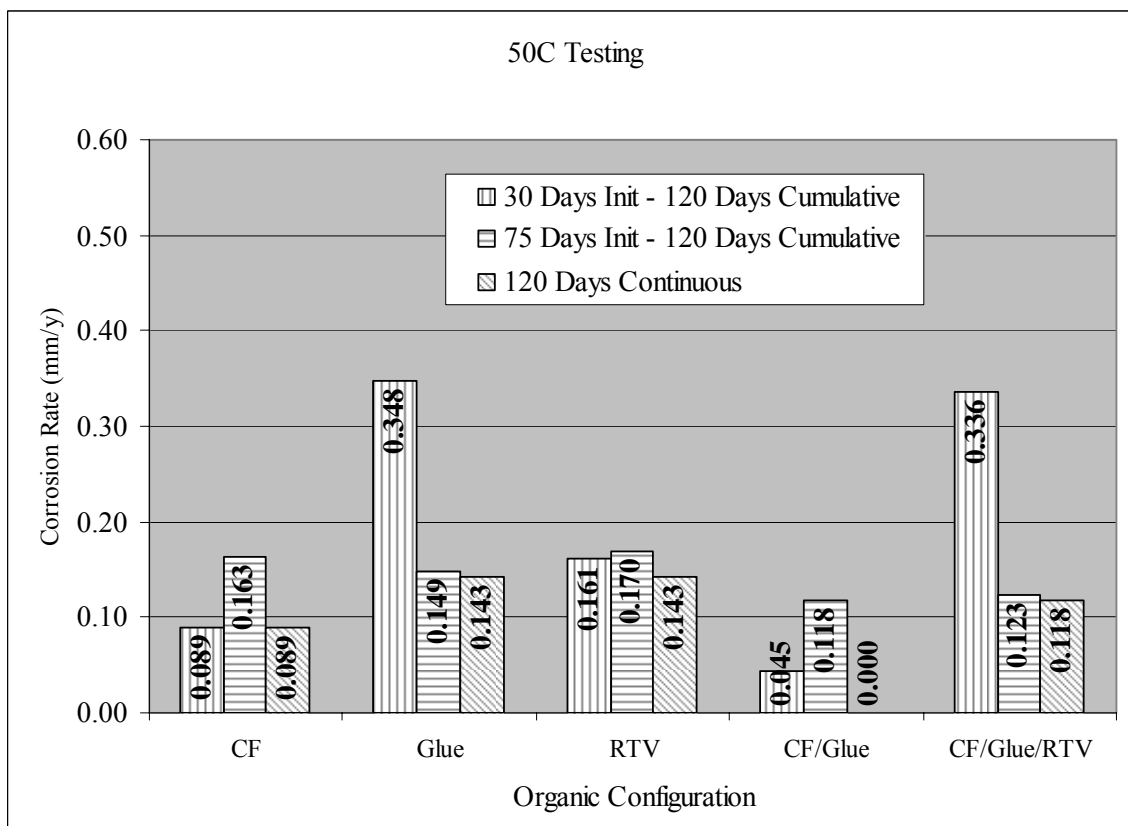


Figure 10: Corrosion Rates for Lead Coupons Exposed to Condensed Water Cells at 50°C for Re-Exposed Coupons and Continuously Exposed 120-Day Coupons

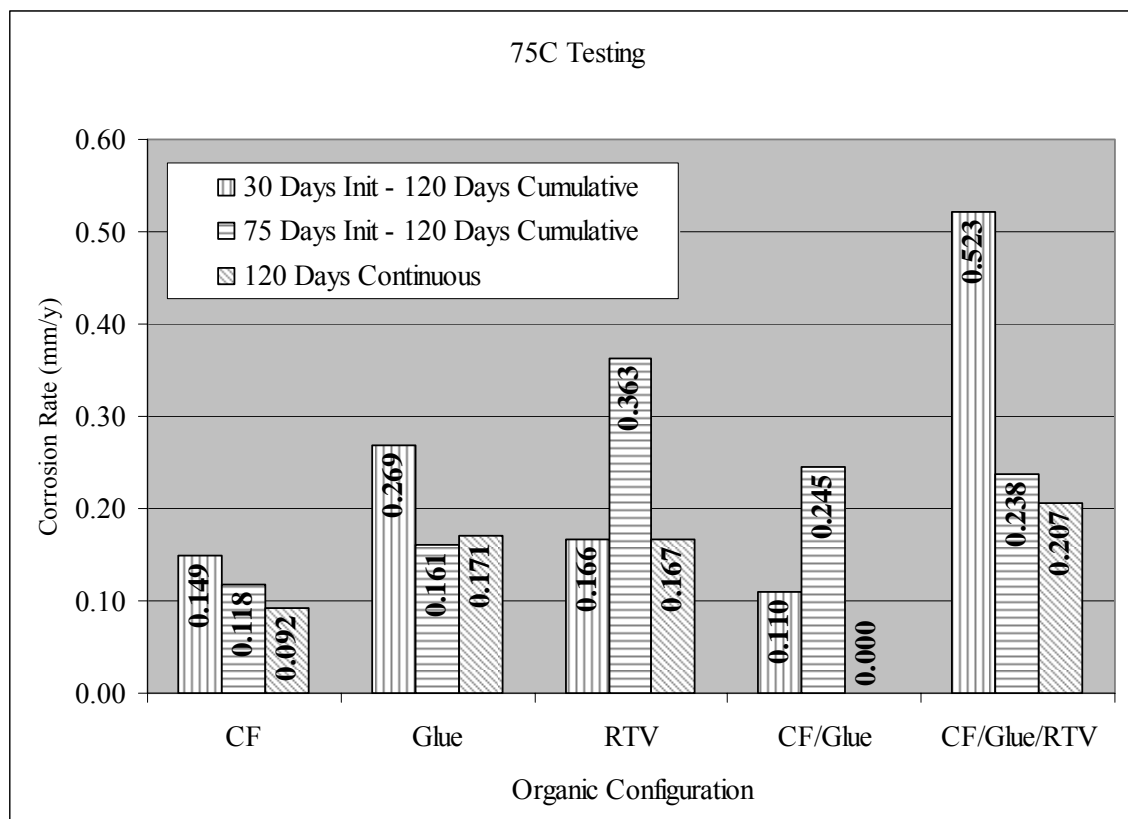


Figure 11: Corrosion Rates for Lead Coupons Exposed to Condensed Water Cells at 75°C for Re-Exposed Coupons and Continuously Exposed 120-Day Coupons

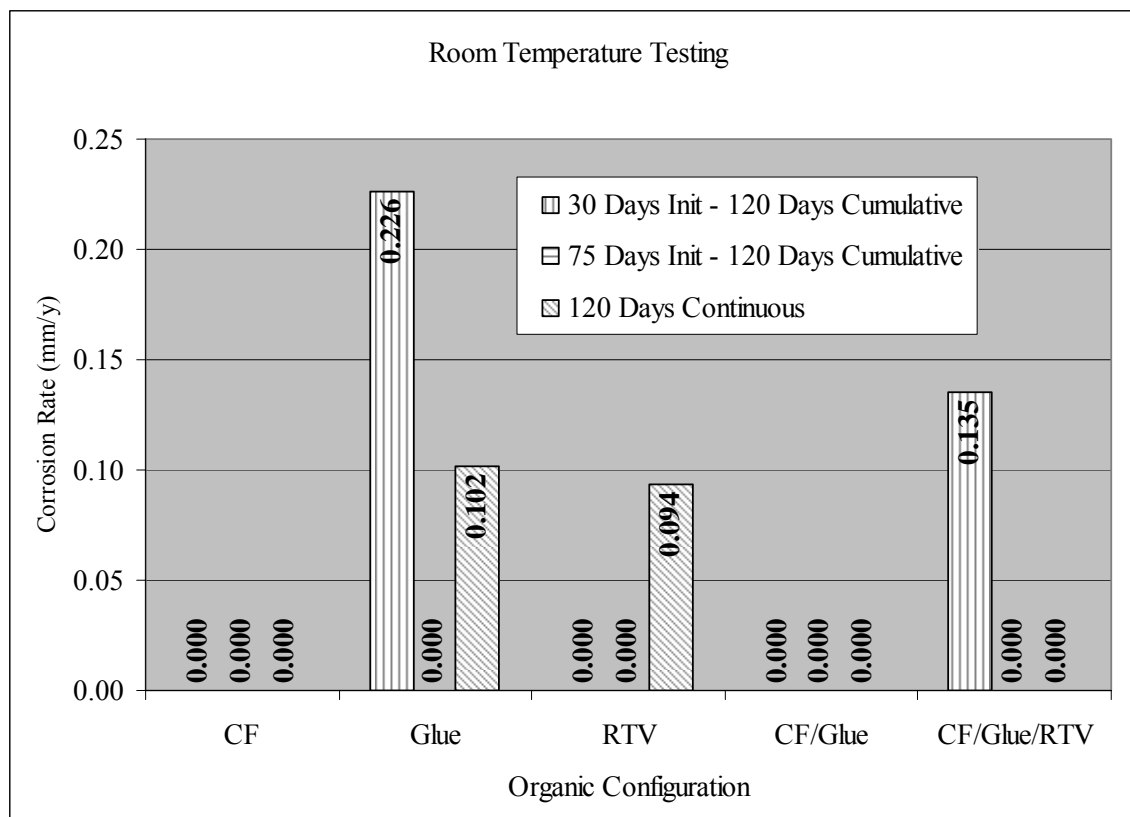


Figure 12: Corrosion Rates for Lead Coupons Exposed to Ambient Humidity Cells at Room Temperature for Re-Exposed Coupons and Continuously Exposed 120-Day Coupons

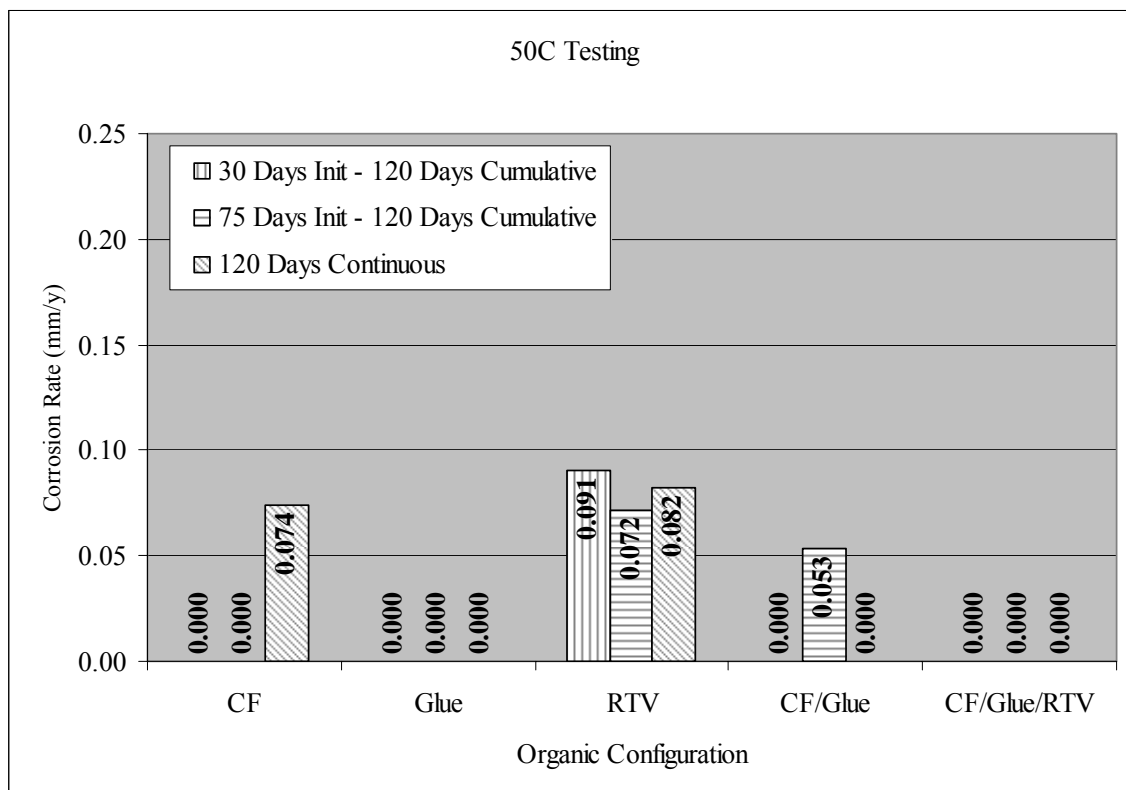


Figure 13: Corrosion Rates for Lead Coupons Exposed to Condensed Water Cells at 50°C for Re-Exposed Coupons and Continuously Exposed 120-Day Coupons

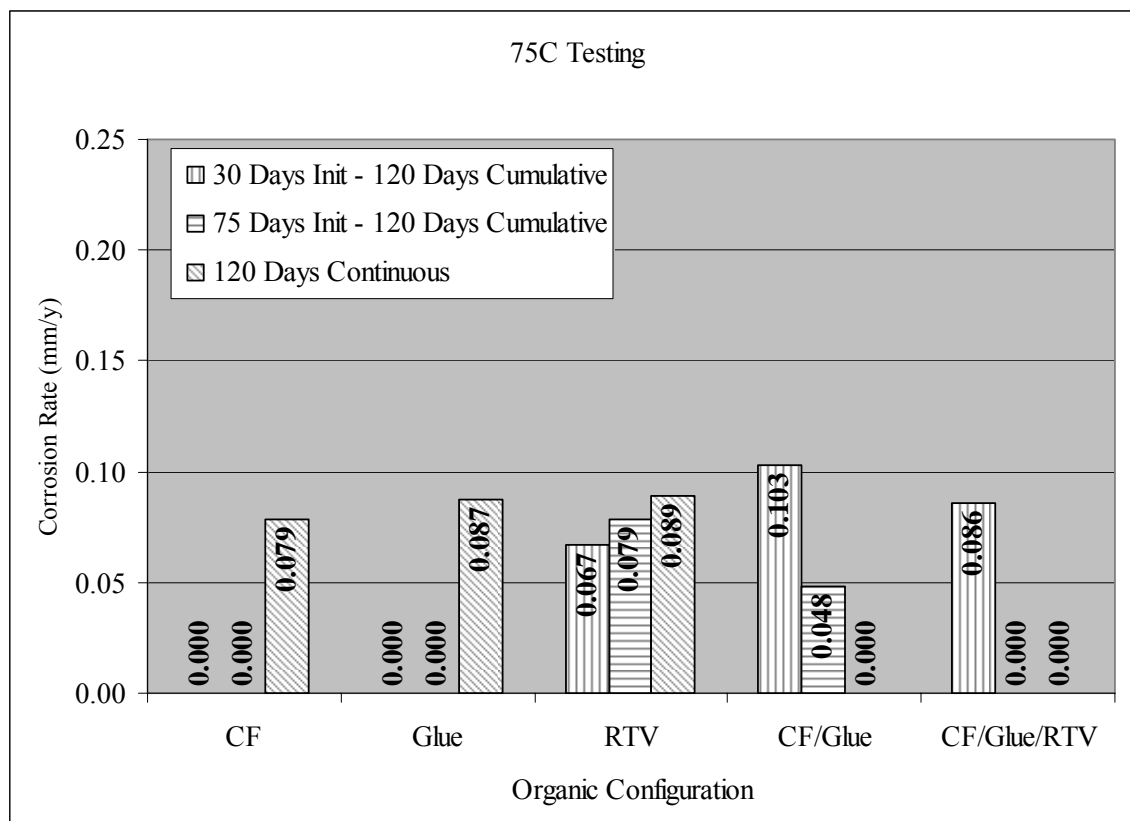


Figure 14: Corrosion Rates for Lead Coupons Exposed to Condensed Water Cells at 75°C for Re-Exposed Coupons and Continuously Exposed 120-Day Coupons